HHS Public Access

Author manuscript

Clin Immunol. Author manuscript; available in PMC 2016 December 28.

Published in final edited form as:

Clin Immunol. 2016 August ; 169: 58–68. doi:10.1016/j.clim.2016.05.011.

Heightened cleavage of Axl receptor tyrosine kinase by ADAM metalloproteases may contribute to disease pathogenesis in SLE

Jacob J. Orme[a], **Yong Du**[a,c], **Kamala Vanarsa**[a,c], **Jessica Mayeux**[a], **Li Li**[a], **Azza Mutwally**[a], **Cristina Arriens**[a], **Soyoun Min**[a], **Jack Hutcheson**[a], **Laurie S. Davis**[a], **Benjamin F. Chong**[b], **Anne B. Satterthwaite**[a], **Tianfu Wu**[a,c], and **Chandra Mohan**[a,c,*]

[a]The Department of Internal Medicine, Rheumatic Diseases Division, University of Texas Southwestern Medical Center, Dallas, TX 75390, United States

[b]The Department of Dermatology, University of Texas Southwestern Medical Center, Dallas, TX 75390, United States

[c]The Department of Biomedical Engineering, University of Houston, Houston, TX 77204-5060, United States

Abstract

Systemic lupus erythematosus (SLE) is characterized by antibody-mediated chronic inflammation in the kidney, lung, skin, and other organs to cause inflammation and damage. Several inflammatory pathways are dysregulated in SLE, and understanding these pathways may improve diagnosis and treatment. In one such pathway, Axl tyrosine kinase receptor responds to Gas6 ligand to block inflammation in leukocytes. A soluble form of the Axl receptor ectodomain (sAxl) is elevated in serum from patients with SLE and lupus-prone mice. We hypothesized that sAxl in SLE serum originates from the surface of leukocytes and that the loss of leukocyte Axl contributes to the disease. We determined that macrophages and B cells are a source of sAxl in SLE and in lupus-prone mice. Shedding of the Axl ectodomain from the leukocytes of lupus-prone mice is mediated by the matrix metalloproteases ADAM10 and TACE (ADAM17). Loss of Axl from lupus-prone macrophages renders them unresponsive to Gas6-induced anti-inflammatory signaling in vitro. This phenotype is rescued by combined ADAM10/TACE inhibition. Mice with Axl-deficient macrophages develop worse disease than controls when challenged with anti-glomerular basement membrane (anti-GBM) sera in an induced model of nephritis. ADAM10 and TACE also mediate human SLE PBMC Axl cleavage. Collectively, these studies indicate that increased metalloprotease-mediated cleavage of leukocyte Axl may contribute to end organ disease in lupus. They further suggest dual ADAM10/TACE inhibition as a potential therapeutic modality in SLE.

*Corresponding author at: Department of Biomedical Engineering, SERC 2004, 3605 Cullen Blvd, Room 2004, Houston, TX 77204-5060, United States. cmohan@Central.UH.EDU (C. Mohan).

Appendix A. Supplementary data

Supplementary data to this article can be found online at http://dx.doi.org/10.1016/j.clim.2016.05.011.

Keywords

SLE; Lupus; Axl; Macrophages

1. Introduction

Systemic lupus erythematosus (SLE) is a group of systemic autoimmune disorders characterized by anti-nuclear antibodies (ANA), rashes and photosensitivity, joint inflammation, nephritis, and other clinical criteria. SLE develops through the breakdown of three major checkpoints: adaptive immune tolerance, peripheral innate immune responsiveness, and end-organ inflammation [1]. Adaptive immune dysfunction produces autoantibodies leading to immune complex formation and deposition in the skin, joints, and kidneys. Innate immunity plays an important role in determining disease severity and progression [2]. Factors and pathways that modulate innate immunity impact the course of disease, particularly in end organ systems where most major, life-threatening disease manifestations occur. We focus here on the Axl receptor tyrosine kinase pathway.

Axl is a member of the TAM family of receptor tyrosine kinases. Axl engagement by its ligand Gas6 causes receptor homodimerization, autophosphorylation, and downstream signaling. Axl and other TAM family members are well-studied in malignancy but also play significant roles in immunity [3–8]. Among immune cells, Axl mRNA expression is highest in macrophages. Axl expression is also reported in some dendritic cells, γδT cells, fibroblasts, CD25+ T cells, and B1a B cells [9].

Disturbance of TAM family function contributes to autoimmunity. TAM family triple knockout mice develop severe systemic autoimmunity, and two members have been implicated directly in autoimmunity [10]. The TAM family member Mer aids in the clearance of apoptotic cells that may otherwise exacerbate inflammation and autoimmunity [11,12]. Further, Axl knockout mice exhibit worse inflammation and demyelination than normal controls in induced experimental autoimmune encephalomyelitis (EAE) [13].

Two major functions of Axl may influence SLE. First, Gas6-stimulated Axl in the kidney is necessary for renal mesangial cell proliferation, which contributes to nephritis [14–17]. Second, Axl signaling blocks the expression of inflammatory cytokines through the induction of Twist, a transcriptional inhibitor, in macrophages [18]. We and others quantified soluble Axl (sAxl) in the serum of SLE patients and healthy controls [19–21]. Patients with active SLE exhibit significantly elevated sAxl versus healthy controls and patients with inactive SLE. Others have proposed modulation of the Axl tyrosine kinase pathway as a new target for SLE, but no feasible mechanism has been determined [22]. We hypothesized that leukocyte Axl is cleaved in lupus, abrogating anti-inflammatory signaling and contributing to the disease.

In the present study we determined that macrophages and B cells are a source of serum sAxl in human SLE and in lupus-prone mice. We further investigated the mechanism of leukocyte Axl loss and its phenotypic effects on lupus. In particular, we found that shedding of the Axl ectodomain from leukocytes is mediated by the proteases ADAM10 and TACE. Further, loss

of Axl from mouse macrophages accentuates inflammation in vitro as well as in vivo in a mouse model of antibody-mediated acute kidney damage, anti-glomerular basement membrane disease (anti-GBM).

2. Materials and methods

2.1. Animals

Congenic control (C57BL/6 or B6), $Axl^{-/-}$, Mrl-lpr, BXSB, and NZM2410 mice were purchased from the Jackson Laboratory (Bar Harbor, ME) or Taconic Farms (Hudson, NY). B6·Sle1 [23], B6·Sle3 [24], B6·Yaa [25], B6.$Lyn^{-/-}$ [26], and BWF1 [27] mice were bred in our mouse colony. Mice used for this study were 3 to 8 month old males and females maintained in a stress-free environment. The Animal Care and Use Committee at the University of Texas Southwestern Medical Center approved all experiments using mice.

2.2. Enzyme-linked immunosorbent assay (ELISA)

Human and mouse sera were probed for sAxl using mouse (R&D Systems, Minneapolis, MN) or human (Raybiotech, Norcross, GA) Axl ELISA kits per the manufacturers' protocols. Sera were diluted 1:100 in a serum diluent (2% BSA, 3 mM EDTA, 0.05% Tween-20) for probing. Total IgM and IgG (Bethyl Laboratories, Montgomery, TX) as well as anti-DNA antibodies were detected by ELISA as previously published [28].

2.3. Bone marrow-derived macrophages

L-cell supernatant was prepared by growing L929 cells in flasks (~20 ml DMEM with 10% FBS, 1% glutamine, 1% HEPES, 1% Pen/Strep) to confluence (3–5 days). Cultures were then split 5×, grown 7 days, and supplemented with 10 ml DMEM with 10% FBS, 1% glutamine, 1% HEPES, and 1% Pen/Strep. After 7 additional days supernatant was filtered and frozen (0.4 μm filters). Bone marrow-derived macrophages (BMDM) were prepared by dissection and flushing of tibias using ~3 ml BM25 media (DMEM with 10% FBS, 25% L supernatant, 5% horse serum, 1% glutamine, 1% sodium pyruvate, and 1% Pen/Strep) into 10 cm untreated petri dishes (final volume 10 ml). Cultures were incubated at 37 ° C in 5% CO_2 for 3 to 4 days and 5 ml media was replenished with new BM25. At day 7 or 8, media was aspirated and replaced with 5 ml BM15 media (DMEM with 10% FBS, 15% L supernatant, 5% horse serum, 1% glutamine, 1% sodium pyruvate, and 1% Pen/Strep). Plates were then scraped and split for propagation and supplemented with additional BM15 media. Cells were allowed 2 to 3 days reequilibration before any treatment or freezing.

2.4. Cell acquisition, treatment, staining, and sorting

Collection of peripheral blood from consented human subjects was overseen and approved by the University of Texas Southwestern Medical Center Institutional Review Board. Blood was centrifuged to isolate serum from whole blood. Peripheral blood mononuclear cells (PBMCs) were isolated by density-gradient centrifugation over Ficoll. Cells were lysed for Western blot analysis, treated, or stained for flow cytometry assays as described in the text. Mouse splenocytes were collected using standard protocols.

Splenocytes were cultured in RPMI with 10% FBS, 50 kU/l penicillin, 50 kU/l streptomycin, and 2 mM glutamine. Bone marrow-derived macrophages were cultured in DMEM supplemented with glutamine, 10% FBS, 5% horse serum, penicillin/streptomycin, and short-term 25% and long-term 15% L929 supernatant [29]. For ADAM10 and TACE inhibition studies, cells were treated with DMSO vehicle control, 50 μM GI254023X (OKeanos, China), 50 μM TAPI-0 (Santa Cruz Biotech, Santa Cruz, CA), or both 50 μM GI254023X and 50 μM TAPI-0 for 24 h. For Gas6 stimulation studies, splenocytes were cultured at 2 million cells/ml and treated with either 1 ng/ml LPS alone (Sigma, St. Louis, MO) or 1 ng/ml LPS plus 400 ng/ml Gas6 (R&D Systems, Minneapolis, MN) for 24 h. B cells were purified from bulk splenocytes by MACS purification (Milltenyi, San Diego, CA) and treated with 1 μg/ml LPS for 24 h before being treated with 400 ng/ml Gas6 or vehicle control over 24 h.

Anti-Axl (LifeSpan BioSystems, Seattle, WA), anti-*p*-Axl (R&D Systems, Minneapolis, MN), and rabbit isotype control (Becton Dickenson, Franklin Lakes, NJ) antibodies were conjugated to Alexa 555® using the APEX™ Alexa Fluor® 555 Antibody Labeling Kit (Invitrogen, Carlsbad, CA) following the manufacturer's protocol. Additional anti-human Axl PE and anti-mouse PE conjugates were used to stain for flow cytometry (R&D Systems, Minneapolis, MN). Additional antibodies used for flow cytometry were FITC CD14, FITC CD4, PE-Cy5 CD4, PE-Cy7 B220, APC CD19, and APC-Cy7 CD11b (Becton Dickenson, Franklin Lakes, NJ); FITC CD3 and APC CD11c (eBiosciences, San Diego, CA). Flow cytometry was performed after the cells were fixed and was gated using forward (FSC) and side (SSC) scatter to isolate live cells using FlowJo (Treestar, Ashland, OR).

2.5. Histopathology

Spleens and kidneys were isolated and prepared for histological analysis by lateral dissection and fixation in OCT medium prior to freezing. Specimens were sectioned (3–5 mm) and stained with appropriate antibodies (Rabbit anti-Axl, LifeSpan BioSystems, Seattle, WA; Alexa 488® Goat anti-Rabbit IgG, Life Technologies, Carlsbad, CA). Slides were fixed with DAPI-containing fixative prior to imaging.

2.6. Western blot analysis

Human PBMC and mouse spleen samples were isolated, lysed, and subjected to SDS-PAGE and transferred to nitrocellulose paper according to standard procedures. Blots were probed with primary antibodies against Axl (LifeSpan BioSystems, Seattle, WA), Y779-phosphorylated Axl (R&D Systems, Minneapolis, MD), GAPDH (Cell Signal, Danvers, MA), α-Tubulin (Cell Signal, Danvers, MA), ADAM10 (R&D Systems, Minneapolis, MN), and TACE (Santa Cruz, Santa Cruz, CA) and subsequently probed with secondary HRP-linked antibodies (GE Healthcare, Fairfield, CT). Bands were visualized with ECL substrate.

2.7. RT-PCR

RNA was extracted from tissue and reverse-transcribed to produce cDNA using standard protocols. cDNA was detected on the Biorad CFX96 Real Time PCR system with SybrGreen® (Biorad, Hercules, CA) using *Axl* (For: 5′-aaccttcaactcctgccttctcg-3′ Rev: 5′-cagcttctccttcagctcttcac-3′), *Cyclophilin* A (For: 5′-gcagacaaagttccaaagacag-3′ Rev: 5′-

cattatggcgtgtaaagtcacc-3′), *Twist* (For: 5′-ggacaagctgagcaagattca-3′ Rev: 5′-cggagaaggcgtagctgag-3′), *Il6* (For: 5′-ctgcaaga gacttccatccagtt-3′ Rev: 5′-gaagtagggaaggccgtgg-3′), and *TNF* (For: 5′-ttctgtctactgaacttcggggtgatcggtcc −3′ Rev: 5′-gtatgagatagcaaatcggctga cggtgtggg-3′) probes. Each sample was normalized to Cyclophilin A control using ΔCt to compute relative expression.

2.8. Anti-GBM disease

Anti-glomerular basement membrane (GBM) disease was induced in mice according to previously-described methods (Fig. 5A, D) [30]. At day (−5), mice were inoculated intraperitoneally with 225 μl of a mixture of 100 μl complete Freund's adjuvant (CFA, Sigma, St. Louis, MO), 100 μl PBS, and 25 μl 10 mg/dl rabbit IgG (Sigma, St. Louis, MO) mixed in Micro-Mate® interchangeable hypodermic syringes (Popper & Sons, NY) with Discofix® 3-way stopcock (B. Braun, PA). On day 0 or 1, mice were inoculated intravenously (tail vein injection) with mouse anti-rabbit glomerular basement membrane serum. This inoculation is dosed by weight at 150 μl per 20 g animal. In a variant of anti-GBM disease, 10^7 bone marrow-derived macrophages (BMDM) are introduced by tail vein injection at day 0 in addition to the other injections to induce disease.

2.9. Assays of kidney function

Serum creatinine was measured using a serum creatinine colorimetric assay kit (Cayman, Ann Arbor, MI) following the manufacturer's protocol. Urine protein was measured in a 96-well plate assay using Pierce® BCA Protein Assay (Thermo Scientific, Rockford, IL) following the manufacturer's protocol.

2.10. Statistical procedures

p values were not otherwise noted were determined using a student's *t* test using GraphPad® Prism software. Significance cutoffs for *p* values were set at 0.05. For Western Blot analysis, bands were quantified using ImageJ®. For comparison purposes in Fig. 1, relative densities were averaged among healthy controls. For statistical comparisons of flow cytometry plots, Mean Fluorescent Intensity units (MFI) were generated and a ratio of Axl staining to Isotype control staining was calculated.

2.11. Human subjects

Collection of peripheral blood from consented human subjects was overseen and approved by the University of Texas Southwestern Medical Center Institutional Review Board (IRB). Controls were matched where possible by age, gender, and ethnicity (see Supplemental Table 1).

2.12. Supplemental figures

Supplemental figures are available in the online edition of this manuscript. Additional data is available in the related Data in Brief article, Ref [31].

3. Results

3.1. Human PBMC Axl loss correlates with serum sAxl in SLE

We observed that cleaved serum Axl ectodomain (sAxl) is elevated in the blood of patients with active SLE (Fig. 1A, see also Supplemental Table 1). This finding has been previously shown by others [19,20]. Renal mesangial cells express Axl in nephritis and were previously posited as a source of sAxl in SLE. This explanation is unsatisfactory both because mesangial cell Axl signaling is intact in nephritis (see Ref [31], Fig. 1) and because ADAM10, the protease implicated in Axl cleavage, is not expressed in SLE mesangial cells [32]. We hypothesized that Axl-expressing leukocytes may shed the Axl ectodomain in SLE. Consistent with this, we found that peripheral blood mononuclear cell (PBMC) extracts from two panels of SLE patients exhibited significantly reduced Axl ectodomain than matched healthy controls (Fig. 1B–D). Work by previous groups suggested that monocytes are the major PBMC subset with substantial Axl expression in healthy humans and that monocytes are increased in patients with SLE [33,34]. This combination would predict an increased level of Axl in PBMCs rather than the decrease we observed. The majority of SLE patient PBMCs also lacked activated (i.e. phosphorylated) Axl by Western analysis. Conversely, sera from these patients exhibited significantly elevated sAxl (Fig. 1E). PBMC Axl and serum sAxl in these patients and healthy controls correlated inversely (Fig. 1F). Taken together these data suggest that PBMCs may be a source of sheared sAxl in the blood of patients with SLE.

3.2. Soluble Axl (sAxl) is elevated in the serum of many lupus-prone mouse strains versus healthy B6 controls

Spontaneous lupus-prone mouse models aid in the study of SLE. We collected sera from various aged lupus-prone mouse strains including Mrl-lpr, BWF1, B6·Sle1, B6·Sle1.Sle2.Sle3, B6·Sle3, B6·Sle1.Sle3, B6·Sle1.Yaa, and B6.Lyn$^{-/-}$ and quantified serum sAxl by ELISA. Lupus-prone strains exhibited elevated sAxl, suggesting this phenomenon is common to both human SLE and spontaneous lupus-prone mice (Fig. 2A). The absolute differences in serum sAxl are approximately twofold, which was consistent across strains. While a low-magnitude increase in circulating Axl may or may not affect Gas6 binding to intact receptors, the functional consequence of Axl removal from a small population of cells may be substantial. Sera from young lupus-prone strains do not exhibit elevated sAxl (see Supplemental Fig. 1A).

3.3. CD11b+ and CD19+ leukocytes from lupus-prone mice lose surface Axl, abrogating signaling

To confirm that leukocytes from lupus-prone mice shed Axl, we obtained sections of healthy and lupus-prone mouse spleens for immunohistochemistry (IHC). We stained with DAPI and anti-Axl antibody. Healthy B6 mouse splenocytes exhibited surface Axl staining but lupus-prone mouse splenocytes did not (Fig. 2B, representative of 3 experiments).

To further confirm Axl ectodomain loss and diminished Axl activation we isolated spleens from six month-old healthy control B6 and diseased lupus-prone Mrl-lpr mice and extracted protein for analysis by Western blot. Splenocytes from diseased Mrl-lpr mice show lower

levels of total Axl and active Y779-phosphorylated Axl than healthy control B6 splenocytes (Fig. 2C, $p = 0.001$ and 0.0015 on densitometry).

While these data suggest that SLE leukocyte Axl loss occurs, they do not pinpoint which cells lose Axl in SLE. To this end, we isolated splenocytes from four-month-old healthy B6 mice and diseased B6·Sle1.Yaa lupus-prone mice and stained with anti-Axl or isotype control antibody for analysis by flow cytometry. Healthy B6-derived CD11b+ and CD19+ splenocytes expressed Axl, whereas healthy B6 CD4+ and CD8+ splenocytes did not. CD11b+ and CD19+ diseased splenocytes from lupus-prone mice were negative for Axl staining (Fig. 2D, representative of three experiments, see Supplemental Table 2). In contrast, young B6·Sle1.Yaa splenocytes express equivalent surface Axl to healthy controls (see Supplemental Fig. 1C). This suggests that macrophages and B cells shed Axl ectodomain in SLE. RT-PCR analysis did not reveal any difference in Axl mRNA expression between lupus-prone and healthy mouse splenocytes, suggesting that leukocyte Axl loss is due to cleavage rather than reduced mRNA levels (Fig. 2E, representative of 3 experiments). This unchanged Axl mRNA expression was also observed in younger, non-diseased mice (see Supplemental Fig. 1B). In another experiment, splenocytes from four month-old female disease-transitioning B6·Sle1 mice but not healthy B6 mice showed a partial loss of Axl in these same cell types (data not shown). It is possible that leukocyte Axl shedding progresses with disease. Indeed, cultured BMDM from the same strain of lupus-prone mice express basal Axl identical to B6 BMDM by flow cytometry (see Supplemental Fig. 2A). Thus Axl shedding from the macrophages in lupus likely occurs in the periphery with progression of disease.

Taken together, our expression studies indicate that elevated serum sAxl is common to SLE patients and murine lupus. They further indicate that B cells and macrophages are a source of shed serum soluble Axl in lupus-prone mice. Decreased Axl autophosphorylation confirms that diminished receptor function accompanies the loss of Axl ectodomian. Reduced surface levels of Axl in lupus-prone mouse leukocytes are not due to reduced mRNA levels. We next sought to determine the cause and consequences of Axl ectodomain shedding in SLE.

3.4. Cell surface matrix metalloproteases ADAM10 and TACE (ADAM17) mediate Axl cleavage from SLE leukocytes

What causes Axl ectodomain shedding in SLE but not healthy control leukocytes? Previous reports assert that Axl is cleaved by matrix metalloprotease ADAM10 (A Disintegrin and Metalloproteinase domain-containing protein 10), leaving a signaling-incompetent Axl receptor stump [35–37]. ADAM10 had not previously been directly implicated in SLE but is elevated in macrophages in inflammatory conditions. These include macrophages in the synovium of rheumatoid arthritis patients [38], in the cerebrospinal fluid (CSF) of multiple sclerosis patients [39], and in the alveoli of emphysema patients [40]. Closely-related matrix metalloprotease TACE (ADAM17, tumor necrosis factor alpha-converting enzyme) is elevated in SLE leukocytes, and our group and others have shown a number of ADAM10- and TACE-processed proteins to be elevated in SLE, notably CXCL16 and TNF [41–43].

We hypothesized that one or both of these related proteases cleave Axl ectodomain from the surface of SLE leukocytes.

To determine whether these proteases are expressed in SLE leukocytes, we isolated spleens from six month-old healthy control B6 and diseased lupus-prone Mrl-lpr and BWF1 mice as well as from four month-old healthy control B6 and diseased lupus-prone B6·Sle1.Yaa mice. Diseased mouse splenocytes exhibited elevated levels of matrix metalloproteases ADAM10 and TACE (ADAM17) versus age-matched healthy B6 controls (Fig. 3A).

The presence of both ADAM10 and TACE on SLE leukocytes does not confirm a role in SLE leukocyte Axl cleavage. While a specific ADAM10-mediated Axl cleavage site has been identified (^{432}QPLHHLVSEPPPRA^{446}), no such site has been found or predicted for TACE [35]. However, TACE and ADAM10 frequently cleave overlapping substrates. We hypothesized that both proteases may synergistically cleave Axl in SLE, and there is indeed evidence for such cooperativity in the published literature [44].

To determine whether ADAM10 or TACE is primarily responsible for Axl cleavage in SLE leukocytes, we isolated lupus-prone splenocytes and treated with an ADAM10-specific inhibitor GI254023, a TACE-specific inhibitor TAPI-0, or both inhibitors combined in vitro. Each inhibitor alone only slightly increased surface Axl staining, whereas treatment with both inhibitors rescued Axl expression on CD11b+, B220+, and CD11c+ splenocytes (Fig. 3B, representative of four experiments). In separate experiments, B6 splenocytes did not change Axl surface expression on protease inhibitor treatment (see Supplemental Fig. 3). Similarly, B6 splenocytes do not shed detectable amounts of Axl in vitro (see Fig. 4A). B6·Sle1.Yaa splenocytes do shed Axl, which is halted by inhibitor treatment. Taken together, these data suggest that both proteases act synergistically to cleave surface Axl on SLE leukocytes.

3.5. Lupus-prone splenocytes fail to respond to Gas6 stimulation but are rescued by combined ADAM10 and TACE inhibition

While the foregoing data confirm the mechanism of Axl ectodomain cleavage in SLE, they do not indicate what, if any, significance Axl cleavage has in disease pathogenesis. In macrophages, Gas6-stimulated Axl signaling normally represses inflammatory cytokine expression by induction of transcription factor/inhibitor Twist [45]. We hypothesized that ADAM10- and TACE-mediated Axl cleavage in lupus-prone immune cells inactivates this anti-inflammatory pathway and contributes to immune cell dysfunction in lupus.

To determine whether Axl loss affects Twist induction in SLE leukocytes, we isolated splenocytes from B6, B6·Sle1.Yaa, and B6.Axl$^{-/-}$ mice and treated them with low-dose LPS control or combined low-dose LPS plus Axl ligand Gas6 for 24 h. We then isolated cDNA and compared *Twist* expression by RT-PCR. Twist is normally induced in macrophages on Gas6 treatment and blocks transcription of NFκB targets. As expected, neither lupus-prone B6·Sle1.Yaa nor B6.Axl$^{-/-}$ splenocytes upregulated Twist in response to Gas6 stimulation (Fig. 4B). We then pretreated splenocytes with both GI254023 and TAPI-0 to inhibit ADAM10- and TACE-mediated Axl cleavage, respectively, prior to Gas6 stimulation. SLE splenocytes but not wild-type or Axl-deficient B6 splenocytes showed restored Gas6-

stimulated Twist induction after combined ADAM10/TACE protease inhibitor treatment (Fig. 4C, D). As previously mentioned, Twist blocks inflammation by inhibiting the mRNA expression of inflammatory cytokine genes including interleukin 6 (*Il6*) and tumor necrosis factor alpha (*Tnfa*) [45]. We found that B6·Sle1.Yaa and B6.Axl$^{-/-}$ splenocytes do not downregulate IL6 and *TNF* transcription in the presence of Gas6. However, this phenotype is rescued in B6·Sle1.Yaa splenocytes following combined ADAM10/TACE inhibitor pretreatment (Fig. 4E, F). MACS-sorted macrophages behaved similarly (data not shown).

It is not known whether B cells, like macrophages, also induce Twist expression in response to Gas6 stimulation. To address this, we isolated B cells and treated them with LPS or LPS and Gas6. Gas6 stimulation does marginally upregulate Twist in healthy B cells but not B6·Sle1.Yaa and B6.Axl$^{-/-}$ B cells (see Ref [31], Fig. 2), although to a lesser extent than was observed in splenocytes. Taken together, these results indicate that macrophage Axl loss abrogates an important anti-inflammatory feedback signal and may contribute to the disease.

3.6. Axl-deficient macrophages worsen anti-GBM end organ damage

End-organ damage is the third and final checkpoint failure in SLE pathogenesis. Inflammation in the kidneys (i.e. nephritis) is a leading cause of morbidity and mortality in SLE [46]. Anti-glomerular basement membrane disease (anti-GBM) is a valuable mouse model of nephritis in which rabbit IgG and complete Freund's adjuvant (CFA) are injected into healthy young mice five days prior to tail vein injection of rabbit anti-glomerular basement protein antiserum (Fig. 5A) [30]. Mice develop nephritis over the course of three weeks as marked by elevated serum creatinine (SCr). Although acute anti-GBM disease is distinctly different from spontaneous lupus nephritis, both diseases share downstream molecular pathways [30]. Hence we used anti-GBM-induced nephritis to model end-organ disease.

To determine whether Axl loss contributes to end-organ damage, we induced anti-GBM disease in B6.Axl$^{+/-}$ (het), B6.Axl$^{-/-}$ (ko), and B6.Axl$^{+/+}$ (wt) littermates and followed disease progression. B6.Axl$^{+/-}$ mice exhibited significantly worse nephritis than wild-type B6 control mice as measured by serum creatinine and urine protein (Fig. 5B, C). Most striking was the development of more profound nephritis in heterozygotes than in complete Axl knockouts. We believe this is likely because renal mesangial cell Axl, which is elevated and not cleaved in SLE, may be crucial to the mesangial cell proliferation underlying nephritis (see Ref [31], Fig. 1) [14–17].

We next sought to isolate the effects of macrophage-specific Axl loss in end organ damage. We previously showed in vitro that SLE leukocyte Axl loss abolishes Twist-mediated inflammatory cytokine inhibition (Fig. 4E, F). A variation of the anti-GBM nephritis model allows testing of the phenotypic effects of macrophages in vivo by cell transfer [30]. In brief, as outlined in Fig. 5D, young healthy B6 mice were challenged with intraperitoneal rabbit IgG plus CFA six days prior (D-5) to anti-GBM antibody tail vein injection (D1). On D0, these mice randomly received adoptively-transferred BMDM from either B6.Axl+/+ or B6.Axl$^{-/-}$ donor littermates following which anti-GBM disease was induced. After three weeks, mice receiving Axl-deficient donor BMDM experienced worse end organ damage as measured by serum creatinine and 24-hour urine protein than those receiving B6.Axl+/+

donor BMDM (Fig. 5E, F). B6 recipients of Axl-deficient donor BMDM also exhibited significantly-elevated serum IL-6 levels, suggesting that Axl-deficient macrophages may constitutively secrete IL-6 to contribute to systemic disease (Fig. 5G). A blinded observer was able to identify recipients of Axl-deficient donor BMDM by their appearance, which included hair fraying, hair loss, and crouched habitus (Supplemental Fig. 4). B6 recipients of B6.Axl+/+ donor BMDM did not exhibit these features. B6.Axl$^{-/-}$ BMDM grew identically to B6.Axl+/+ BMDM in vitro, suggesting that these differences were not altered by cell survival.

3.7. Human PBMC Axl is also rescued by combined ADAM10/TACE inhibition

We have shown that human PBMCs shed Axl ectodomain in SLE. We have further shown that this shedding, which also occurs in lupus-prone mice, is mediated by matrix metalloproteases ADAM10 and TACE (ADAM17) and is pathogenic in mouse macrophages in vitro and in vivo. We next sought to determine whether these same proteases are also at work in human SLE leukocytes.

Western blot analysis showed that TACE is significantly elevated and ADAM10 is present in SLE patient PBMC extracts versus healthy controls (Fig. 6A, B). We next treated freshly-isolated PBMCs from SLE patients for 18 h with vehicle control, ADAM10 inhibitor GI254023, TACE inhibitor TAPI-0, or both. Cells were then stained for human Axl and isotype control for analysis by flow cytometry. As with mouse splenocytes, individual protease inhibitor treatment elicited only marginal increases in surface Axl in each patient PBMC sample. Further, combined protease inhibitor treatment elicited greater increases in Axl surface expression. This rescue occurred variably on CD14+ or CD19+ SLE PBMCs or both. CD3+ human PBMCs did not express Axl (Fig. 6C, representative plot of five patients; summarized in Fig. 6D). This variability between patient samples is consistent with our observations in Fig. 1. Taken together with diminished Axl phosphorylation in SLE PBMCs (see Fig. 1B, C), these data suggest that ADAM10 and TACE cleave Axl and abrogate Axl signaling in human SLE PBMCs.

4. Discussion and conclusion

In the present study we observe that SLE patients and lupus-prone mice exhibit increased levels of sheared soluble Axl ectodomain (sAxl) in the blood and reduced surface Axl and active Y779-phosphorylated Axl on immune cells. This occurs despite increased Axl ligand Gas6 in SLE serum [19–21]. We demonstrate that matrix metalloproteases ADAM10 and TACE (ADAM17) cleave surface Axl on CD11b+ or CD14+ and CD19+ lupus leukocytes. Under normal conditions, Axl acts to transduce anti-inflammatory signals in macrophages through Twist-mediated suppression of inflammatory cytokines [18].This represents a part of the innate immune checkpoint, and dysregulation of this system may contribute to the pathology of autoimmune disease. We demonstrate that the loss of surface Axl abrogates Axl-mediated anti-inflammatory activity in vitro and in vivo. Both Axl-deficient and lupus-prone mouse macrophages fail to induce Twist or block expression of IL-6 and TNF-alpha in response to Gas6. Axl-deficient BMDM worsen end organ damage in vivo. To our

knowledge these are the first data to show the functional significance of Axl ectodomain shearing in lupus.

Young disease-transitioning B6·Sle1 mice show partial loss of leukocyte Axl versus B6 controls (data not shown). Further, BMDM from diseased B6·Sle1.Yaa mice do not express detectable levels of ADAM10 and TACE (ADAM17) but do express basal levels of Axl similar to wild type B6-derived BMDM (Supplemental Fig. 2A, B). Thus, leukocyte Axl shearing in SLE appears to occur mainly in the periphery in response to an inflammatory milieu. This is consistent with known upregulation of macrophage proteases in inflammatory conditions [38–40]. We speculate that Axl loss in macrophages may contribute to “flares”—periodic, severe worsening of SLE symptoms with no clear cause—by failing to appropriately rein in inflammatory cytokine secretion. This is supported by multiple reports and our observations correlating serum sAxl levels with disease severity on the SLEDAI (systemic lupus erythematosus disease activity index) scale [19,20].

The loss of Axl from blood monocytes could decrease Axl anti-inflammatory signaling in two ways. First, cleavage of cell-surface Axl abrogates Axl signaling through the remaining “stump” receptor. This “cis” suppression of Axl anti-inflammatory signaling on macrophages is supported by our studies outlined here. Second, this cleavage produces a decoy receptor “sink” that may block Gas6 signaling in other cells. This “trans” suppression would affect cells in which Axl and/or other Gas6 receptors like Mer and Tyro3 remain intact. Because Gas6 has higher binding affinity to Axl than to other receptors [5], this sink may effectively abrogate TAM receptor signaling pathways in other cells. Additional study will be required to determine whether “trans” sAxl effects are physiologically significant (see Ref [31], Fig. 3 for preliminary data).

The consequences of Axl shedding from B cells are less clear. While we show that normal, healthy CD19+ mouse leukocytes express Axl, they upregulate Twist marginally upon Gas6 stimulation (see Ref [31], Fig. 2). It remains to be explored how Gas6-mediated Axl signaling affects B cells normally and in SLE.

Type I interferons (IFN I) are known to be elevated in SLE but do not exert anti-inflammatory effects [47–50]. Many studies have provided explanations for this phenomenon, including activation of different subsets of autoreactive cells [51]. The present study may offer an additional explanation of this phenomenon, as at least part of the IFN I mediated anti-inflammatory effect may be Axl-dependent [18]. Further study is warranted to address this possibility.

Recent interest in sAxl in SLE serum has led to conflicting reports of significant versus insignificant correlation of serum sAxl and disease severity [19–21]. This may be due to variation in patient populations studied. Our patient cohorts in Fig. 1 and others reporting significant correlation of sAxl and disease have generally focused on Hispanic and African American patients and controls, whereas those reporting insignificant correlation comprise mainly European American patients and controls. Different reports also cite significantly decreased or increased Gas6 in severe SLE [14,19–21], although these variations may be due to differences in measuring free versus sAxl-bound Gas6. Most report an increase.

While the Axl ligand Gas6 is elevated in the serum of mice and humans with SLE, its anti-inflammatory activity may be blunted in leukocytes by Axl shearing. Conversely, Gas6 in the kidney contributes to nephritis and inflammation through Axl-mediated mesangial cell proliferation [14–17]. In short, Axl signaling has opposing effects in mesangial cells (pro-disease) versus peripheral leukocytes (anti-inflammatory). Thus an Axl kinase inhibitor may exacerbate SLE by inhibiting Twist-mediated anti-inflammatory signaling in macrophages while a Gas6 homolog may exacerbate SLE by enhancing mesangial cell proliferation. Matrix metalloprotease inhibition, which would directly increase leukocyte but not mesangial cell Axl signaling, may be a more effective therapeutic intervention.

Matrix metalloprotease inhibitors are increasingly available and tested for other indications in clinical trials. The present study suggests that either ADAM10 or TACE inhibition alone will not maximally restore leukocyte Axl function. We found that lower doses of ADAM10/TACE inhibitors exhibit similarly synergistic upregulation of Axl versus either inhibitor alone by flow cytometry (data not shown). This suggests that the observed Axl rescue is not due to any off-target effects of either inhibitor. Taken together, these data further suggest that dual inhibition using multiple inhibitors or a multi-selective inhibitor that spares other proteases may improve macrophage phenotypes in vivo. Small molecule XL784, for instance, recently completed Phase 2 clinical testing in diabetic nephropathy and selectively inhibits both proteases while sparing other close family members [52]. We previously reviewed how influencing macrophage phenotypes in SLE may offer an effective treatment strategy [53]. Continued investigation into this treatment strategy will be required to confirm these effects.

In conclusion, our results show that SLE macrophage proteases ADAM10 and TACE (ADAM17) shear surface Axl and abrogate anti-inflammatory Gas6-mediated Twist induction. Combined with previous reports, our data suggest that Axl loss may contribute to pathology in some SLE patients. On a broader note, the increased expression of several disease mediators in lupus, including TNF, CXCL16, EGFR ligand, and others may all be the consequence of heightened ADAM metalloproteases in this disease [44]. Thus the study may further suggest the exploration of combined ADAM10/TACE inhibition as a treatment for SLE. Additional study is warranted.

Supplementary Material

Refer to Web version on PubMed Central for supplementary material.

Acknowledgments

We thank Hansaa Abbasi, Lin-chiang Tseng, Gina Aloisio, and Li Li for technical assistance. We are grateful to R&D Systems for the kind gift of PE-conjugated anti-mouse Axl antibody. We further thank the UT Southwestern Animal Resource Center for assistance. Funding support was provided by NIH R01 DK81872.

Abbreviations

ANA	Anti-nuclear antibodies
Axl	Axl tyrosine kinase (UFO)

BMDM	Bone marrow-derived macrophages
GBM	Glomerular basement membrane disease
SLE	Systemic lupus erythematosus
PBMC	Peripheral blood mononuclear cell

References

1. Kanta H, Mohan C. Three checkpoints in lupus development: central tolerance in adaptive immunity, peripheral amplification by innate immunity and end-organ inflammation. Genes Immun. 2009; 10:390–396. [PubMed: 19262576]
2. Orme J, Mohan C. Macrophages and neutrophils in SLE—An online molecular catalog. Autoimmun. Rev. 2012; 11:365–372. [PubMed: 22036828]
3. Cao WM, Murao K, Imachi H, Sato M, Nakano T, Kodama T, Sasaguri Y, Wong NC, Takahara J, Ishida T. Phosphatidylinositol 3-OH kinase-Akt/protein kinase B pathway mediates Gas6 induction of scavenger receptor A in immortalized human vascular smooth muscle cell line. Arterioscler. Thromb. Vasc. Biol. 2001; 21:1592–1597. [PubMed: 11597931]
4. Fridell Y, Jin Y, Quilliam LA, Burchert A, McCloskey P, Spizz G, Varnum B, Der C, Liu ET. Differential activation of the Ras/extracellular-signal-regulated protein kinase pathway is responsible for the biological consequences induced by the Axl receptor tyrosine kinase. Mol. Cell. Biol. 1996; 16:135–145. [PubMed: 8524290]
5. Goruppi S, Ruaro E, Varnum B, Schneider C. Gas6-mediated survival in NIH3T3 cells activates stress signalling cascade and is independent of Ras. Oncogene. 1999; 18:4224. [PubMed: 10435635]
6. Hasanbasic I, Cuerquis J, Varnum B, Blostein MD. Intracellular signaling pathways involved in Gas6-Axl-mediated survival of endothelial cells. Am. J. Physiol. Heart Circ. Physiol. 2004; 287:H1207–H1213. [PubMed: 15130893]
7. Tai K, Shieh Y, Lee C, Shiah S, Wu C. Axl promotes cell invasion by inducing MMP-9 activity through activation of NF-κB and Brg-1. Oncogene. 2008; 27:4044–4055. [PubMed: 18345028]
8. Zhang QK, Boast S, De Los Santos K, Begemann M, Goff SP. Transforming activity of retroviral genomes encoding Gag-Axl fusion proteins. J. Virol. 1996; 70:8089–8097. [PubMed: 8892934]
9. Heng TS, Painter MW, Elpek K, Lukacs-Kornek V, Mauermann N, Turley SJ, Koller D, Kim FS, Wagers AJ, Asinovski N. The immunological genome project: networks of gene expression in immune cells. Nat. Immunol. 2008; 9:1091–1094. [PubMed: 18800157]
10. Lu Q, Lemke G. Homeostatic regulation of the immune system by receptor tyrosine kinases of the Tyro 3 family. Science. 2001; 293:306–311. [PubMed: 11452127]
11. Scott RS, McMahon EJ, Pop SM, Reap EA, Caricchio R, Cohen PL, Earp HS, Matsushima GK. Phagocytosis and clearance of apoptotic cells is mediated by MER. Nature. 2001; 411:207–211. [PubMed: 11346799]
12. Seitz HM, Camenisch TD, Lemke G, Earp HS, Matsushima GK. Macrophages and dendritic cells use different Axl/Mertk/Tyro3 receptors in clearance of apoptotic cells. J. Immunol. 2007; 178:5635–5642. [PubMed: 17442946]
13. Weinger JG, Brosnan CF, Loudig O, Goldberg MF, Macian F, Arnett HA, Prieto AL, Tsiperson V, Shafit-Zagardo B. Loss of the receptor tyrosine kinase Axl leads to enhanced inflammation in the CNS and delayed removal of myelin debris during experimental autoimmune encephalomyelitis. J. Neuroinflammation. 2011; 8
14. Fiebeler A, Park J-K, Muller DN, Lindschau C, Mengel M, Merkel S, Banas B, Luft FC, Haller H. Growth arrest specific protein 6/Axl signaling in human inflammatory renal diseases. Am J. Kidney Dis. 2004; 43:286–295. [PubMed: 14750094]
15. Melaragno MG, Wuthrich DA, Poppa V, Gill D, Lindner V, Berk BC, Corson MA. Increased expression of Axl tyrosine kinase after vascular injury and regulation by G protein-coupled receptor agonists in rats. Circ. Res. 1998; 83:697–704. [PubMed: 9758639]

16. Nagai K, Matsubara T, Mima A, Sumi E, Kanamori H, IEHARA N, Fukatsu A, Yanagita M, Nakano T, Ishimoto Y. Gas6 induces Akt/mTOR-mediated mesangial hypertrophy in diabetic nephropathy. Kidney Int. 2005; 68:552–561. [PubMed: 16014032]
17. Yanagita M, Arai H, Ishii K, Nakano T, Ohashi K, Mizuno K, Varnum B, Fukatsu A, Doi T, Kita T. Gas6 regulates mesangial cell proliferation through Axl in experimental glomerulonephritis. Am. J. Pathol. 2001; 158:1423–1432. [PubMed: 11290560]
18. Sharif MN, Šošić D, Rothlin CV, Kelly E, Lemke G, Olson EN, Ivashkiv LB. Twist mediates suppression of inflammation by type I IFNs and Axl. J. Exp. Med. 2006; 203:1891–1901. [PubMed: 16831897]
19. Ekman C, Jönsen A, Sturfelt G, Bengtsson AA, Dahlbäck B. Plasma concentrations of Gas6 and sAxl correlate with disease activity in systemic lupus erythematosus. Rheumatology. 2011
20. Zhu H, Sun X, Zhu L, Hu F, Shi L, Fan C, Li Z, Su Y. Different expression patterns and clinical significance of mAxl and sAxl in systemic lupus erythematosus. Lupus. 2014
21. Zizzo G, Guerrieri J, Dittman LM, Merrill JT, Cohen PL. Circulating levels of soluble MER in lupus reflect M2c activation of monocytes/macrophages, autoantibody specificities and disease activity. Arthritis Res. Ther. 2013; 15:R212. [PubMed: 24325951]
22. Zagórska A, Través PG, Lew ED, Dransfield I, Lemke G. Diversification of TAM receptor tyrosine kinase function. Nat. Immunol. 2014
23. Morel L, Blenman KR, Croker BP, Wakeland EK. The major murine systemic lupus erythematosus susceptibility locus, Sle1, is a cluster of functionally related genes. Proc. Natl. Acad. Sci. U. S. A. 2001; 98:1787–1792. [PubMed: 11172029]
24. Morel L, Croker BP, Blenman KR, Mohan C, Huang G, Gilkeson G, Wakeland EK. Genetic reconstitution of systemic lupus erythematosus immunopathology with polycongenic murine strains. Proc. Natl. Acad. Sci. U. S. A. 2000; 97:6670–6675. [PubMed: 10841565]
25. Subramanian S, Tus K, Li Q-Z, Wang A, Tian X-H, Zhou J, Liang C, Bartov G, McDaniel LD, Zhou XJ. A Tlr7 translocation accelerates systemic autoimmunity in murine lupus. Proc. Natl. Acad. Sci. U. S. A. 2006; 103:9970–9975. [PubMed: 16777955]
26. Chan VW, Meng F, Soriano P, DeFranco AL, Lowell CA. Characterization of the B lymphocyte populations in Lyn-deficient mice and the role of Lyn in signal initiation and down-regulation. Immunity. 1997; 7:69–81. [PubMed: 9252121]
27. Helyer BJ, Howie JB. Renal disease associated with positive lupus erythematosus tests in a cross-bred strain of mice. Nature. 1963; 197:197.
28. Mohan C, Adams S, Stanik V, Datta SK. Nucleosome: a major immunogen for pathogenic autoantibody-inducing T cells of lupus. J. Exp. Med. 1993; 177:1367–1381. [PubMed: 8478612]
29. Weischenfeldt J, Porse B. Bone marrow-derived macrophages (BMM): isolation and applications. Cold Spring Harb. Protoc. 2008 ((2008) pdb. prot5080).
30. Fu Y, Du Y, Mohan C. Experimental anti-GBM disease as a tool for studying spontaneous lupus nephritis. Clin. Immunol. 2007; 124:109–118. [PubMed: 17640604]
31. Orme JJ, Du Y, Vanarsa K, Mayeux J, Li L, Mutwally A, Arriens C, Min S, Davis LS, Chong BF, Satterthwaite AB, Wu T, Mohan C. Axl is altered in SLE. Clin. Immunol. 2016 (Data in Brief).
32. Gutwein P, Schramme A, Abdel-Bakky MS, Doberstein K, Hauser IA, Ludwig A, Altevogt P, Gauer S, Hillmann A, Weide T, Jespersen C, Eberhardt W, Pfeilschifter J. ADAM10 is expressed in human podocytes and found in urinary vesicles of patients with glomerular kidney diseases. J. Biomed. Sci. 2010; 17
33. Neubauer A, Fiebeler A, Graham D, O'Bryan J, Schmidt C, Barckow P, Serke S, Siegert W, Snodgrass H, Huhn D. Expression of Axl, a transforming receptor tyrosine kinase, in normal and malignant hematopoiesis. Blood. 1994; 84:1931–1941. [PubMed: 7521695]
34. Abbas AR, Wolslegel K, Seshasayee D, Modrusan Z, Clark HF. Deconvolution of blood microarray data identifies cellular activation patterns in systemic lupus erythematosus. PLoS One. 2009; 4:e6098. [PubMed: 19568420]
35. Budagian V, Bulanova E, Orinska Z, Duitman E, Brandt K, Ludwig A, Hartmann D, Lemke G, Saftig P, Bulfone-Paus S. Soluble Axl is generated by ADAM10-dependent cleavage and associates with Gas6 in mouse serum. Mol. Cell. Biol. 2005; 25:9324–9339. [PubMed: 16227584]

36. O'Bryan JP, Fridell Y-W, Koski R, Varnum B, Liu ET. The transforming receptor tyrosine kinase, Axl, is post-translationally regulated by Proteolytic cleavage. J. Biol. Chem. 1995; 270:551–557. [PubMed: 7822279]
37. Wilhelm I, Nagyőszi P, Farkas AE, Couraud P-O, Romero IA, Weksler B, Fazakas C, Dung NTK, Bottka S, Bauer H, Bauer H-C, Krizbai IA. Hyperosmotic stress induces Axl activation and cleavage in cerebral endothelial cells. J. Neurochem. 2008; 107:116–126. [PubMed: 18673450]
38. Van Der Voort R, Van Lieshout AWT, Toonen LWJ, Slöetjes AW, Van Den Berg WB, Figdor CG, Radstake TRDJ, Adema GJ. Elevated CXCL16 expression by synovial macrophages recruits memory T cells into rheumatoid joints. Arthritis Rheum. 2005; 52:1381–1391. [PubMed: 15880344]
39. Kieseier BC, Pischel H, Neuen-Jacob E, Tourtellotte WW, Hartung H-P. ADAM-10 and ADAM-17 in the inflamed human CNS. Glia. 2003; 42:398–405. [PubMed: 12730960]
40. Saitoh H, Leopold PL, Harvey B-G, O'Connor TP, Worgall S, Hackett NR, Crystal RG. Emphysema mediated by lung overexpression of ADAM10. Clin. Transl. Sci. 2009; 2:50–56. [PubMed: 20443867]
41. Huovila A-PJ, Turner AJ, Pelto-Huikko M, Kärkkäinen I, Ortiz RM. Shedding light on ADAM metalloproteinases. Trends Biochem. Sci. 2005; 30:413–422. [PubMed: 15949939]
42. Wu T, Xie C, Wang HW, Zhou XJ, Schwartz N, Calixto S, Mackay M, Aranow C, Putterman C, Mohan C. Elevated urinary VCAM-1,P-selectin, soluble TNF receptor-1, and CXC chemokine ligand 16 in multiple murine lupus strains and human lupus nephritis. J. Immunol. 2007; 179:7166–7175. [PubMed: 17982109]
43. Yamamoto S, Higuchi Y, Yoshiyama K, Shimizu E, Kataoka M, Hijiya N, Matsuura K. ADAM family proteins in the immune system. Immunol. Today. 1999; 20:278–284. [PubMed: 10354553]
44. Pruessmeyer J, Ludwig A. The good, the bad and the ugly substrates for ADAM10 and ADAM17 in brain pathology, inflammation and cancer. Semin. Cell Dev. Biol. 2009; 20:164–174. [PubMed: 18951988]
45. Sosic D, Richardson JA, Yu K, Ornitz DM, Olson EN. Twist regulates cytokine gene expression through a negative feedback loop that represses NF-kappaB activity. Cell. 2003; 112:169–180. [PubMed: 12553906]
46. Cervera R, Khamashta MA, Font J, Sebastiani GD, Gil A, Lavilla P, Mejía JC, Aydintug AO, Chwalinska-Sadowska H, de Ramón E. Morbidity and mortality in systemic lupus erythematosus during a 10-year period: a comparison of early and late manifestations in a cohort of 1,000 patients. Medicine (Baltimore). 2003; 82:299–308. [PubMed: 14530779]
47. Baechler EC, Batliwalla FM, Karypis G, Gaffney PM, Ortmann WA, Espe KJ, Shark KB, Grande WJ, Hughes KM, Kapur V. Interferon-inducible gene expression signature in peripheral blood cells of patients with severe lupus. Proc. Natl. Acad. Sci. U. S. A. 2003; 100:2610–2615. [PubMed: 12604793]
48. Bennett L, Palucka AK, Arce E, Cantrell V, Borvak J, Banchereau J, Pascual V. Interferon and Granulopoiesis signatures in systemic lupus erythematosus blood. J. Exp. Med. 2003; 197:711–723. [PubMed: 12642603]
49. Dall'Era MC, Cardarelli PM, Preston BT, Witte A, Davis JC. Type I interferon correlates with serological and clinical manifestations of SLE. Ann. Rheum. Dis. 2005; 64:1692–1697. [PubMed: 15843451]
50. Tilg H. New insights into the mechanisms of interferon alfa: an immunoregulatory and anti-inflammatory cytokine. Gastroenterology. 1997; 112:1017–1021. [PubMed: 9041265]
51. Banchereau J, Pascual V. Type I interferon in systemic lupus erythematosus and other autoimmune diseases. Immunity. 2006; 25:383–392. [PubMed: 16979570]
52. Williams JM, Zhang J, North P, Lacy S, Yakes M, Dahly-Vernon A, Roman RJ. Evaluation of metalloprotease inhibitors on hypertension and diabetic nephropathy. Am. J. Physiol. Ren. Physiol. 2011; 300:F983.
53. Orme J, Mohan C. Macrophage subpopulations in systemic lupus erythematosus. Discov. Med. 2012; 13:151–158. [PubMed: 22369974]

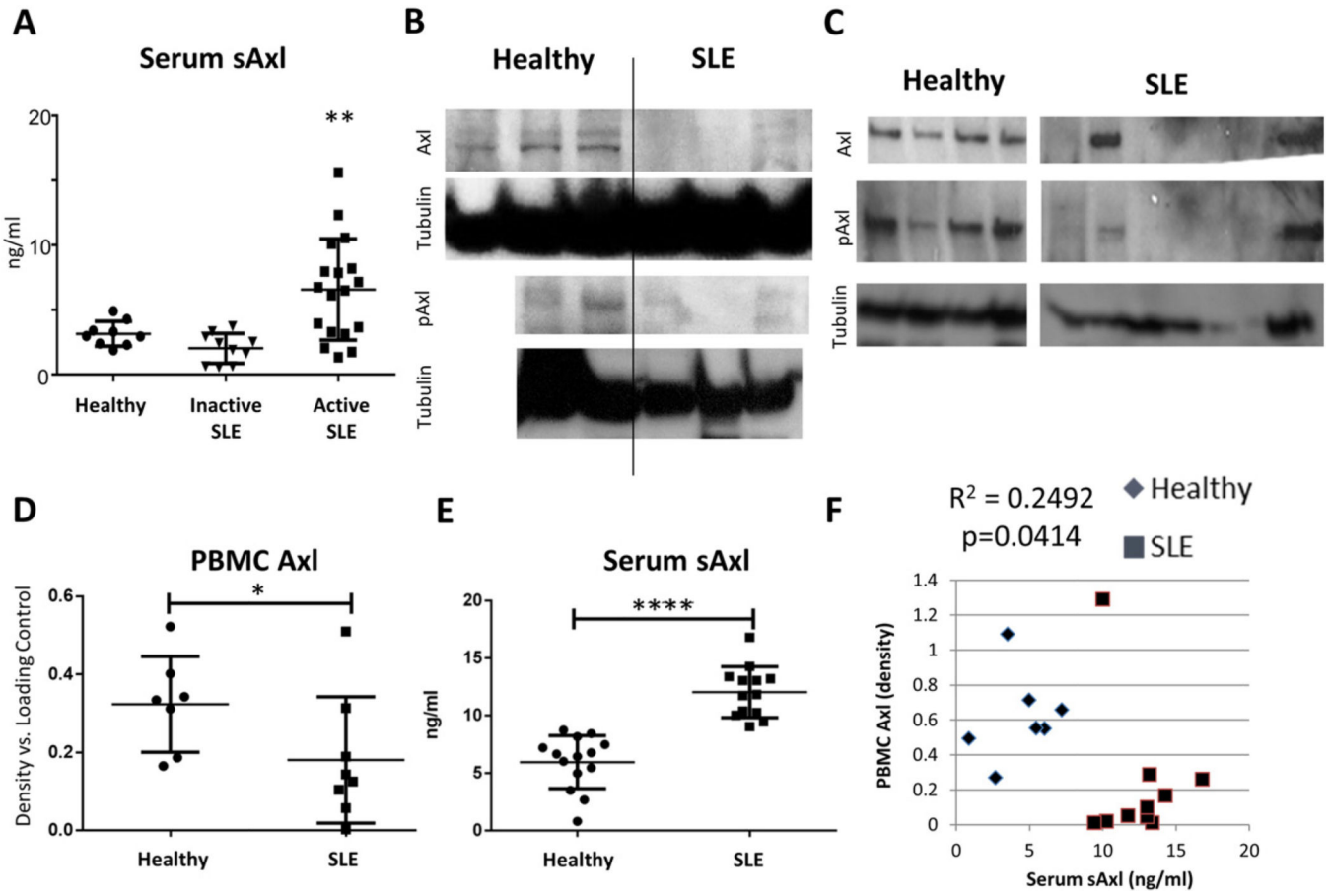

Fig. 1.

SLE PBMC Axl and serum sAxl are inversely proportionate. (A) Soluble Axl was measured by ELISA in the serum of healthy controls ($n = 9$), patients with inactive SLE by clinical score ($n = 10$, SLEDAI ≤ 4), and patients with active SLE by clinical score ($n = 18$, SLEDAI > 4). Patients with active SLE have significantly higher levels of sAxl than healthy controls ($p = 0.0084$) or patients with inactive SLE ($p = 0.0007$). (B, C) PBMCs from two sets of healthy ($n = 3, 4$) and SLE ($n = 3, 7$) subjects were isolated and analyzed for Axl by Western blot. SLE PBMCs showed decreased total Axl ectodomain and pAxl (Y779, activated). (D) Densitometry of Axl versus α-Tubulin loading control was used to quantify the loss of surface Axl on SLE PBMCs versus healthy controls from B and C and plotted in relative units ($p = 0.0398$). (E) ELISA shows a significant increase in serum Axl (sAxl) in the same patients as in D ($p < 0.0001$). (F) Data from D and E correlate inversely with each other ($R^2 = 0.2492$, $p = 0.0414$ by Pearson correlation test). These data suggest that PBMCs may be a source of sheared sAxl in lupus patients. Error bars represent standard deviation. See also Supplemental Table 1.

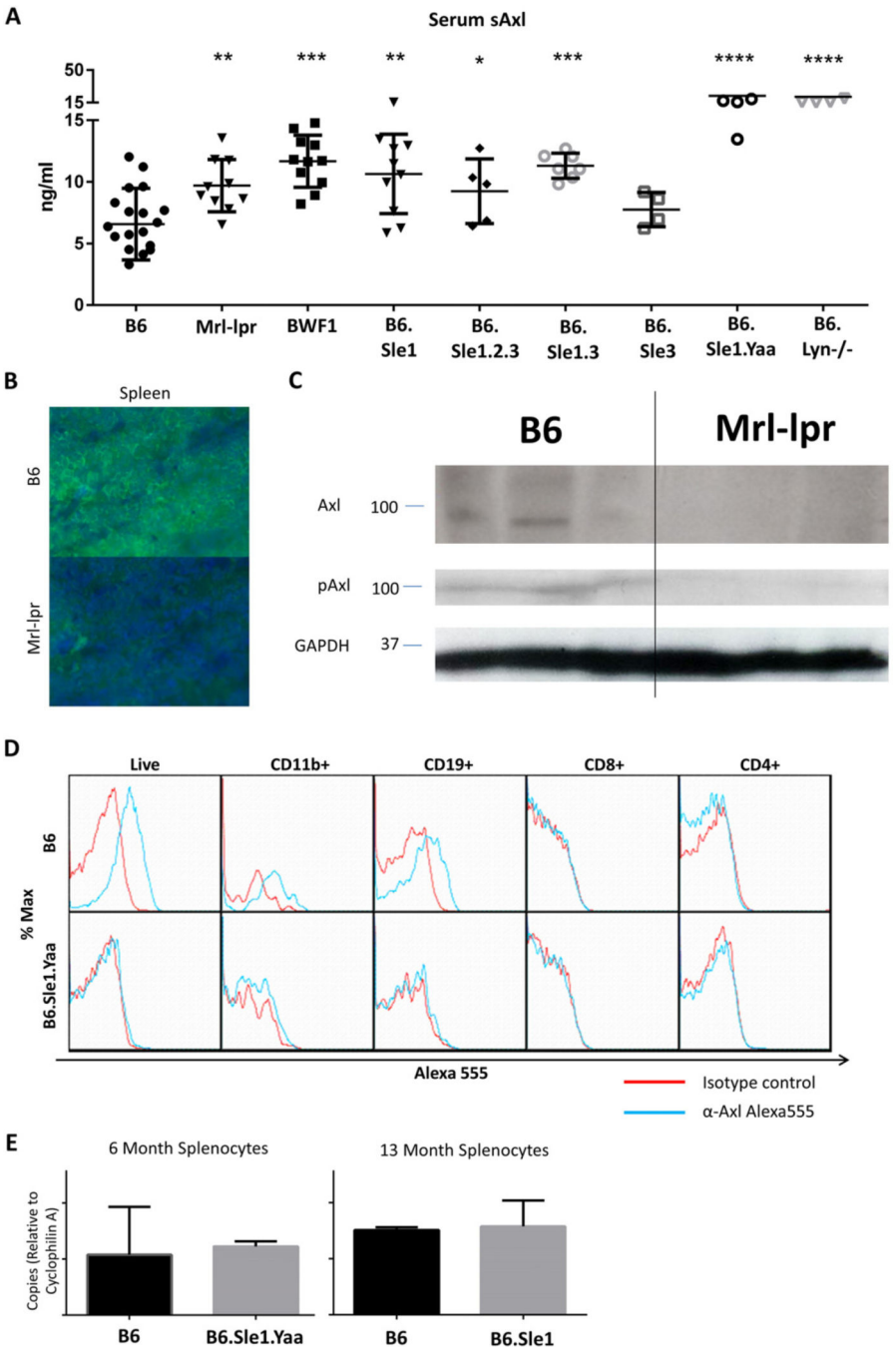

Fig. 2.

Lupus-prone mouse splenocytes lose Axl expression versus healthy controls. (A) Serum Axl is increased in lupus-prone strains versus ≈8-month-old B6 background ($n = 18$). sAxl is significantly higher in Mrl-lpr (≈5 months, $n = 10$, $p = 0.0030$), BWF1 (≈8 months, $n = 11$, $p < 0.0001$), B6·Sle1 (12 months, $n = 10$, $p = 0.0009$), B6·Sle1.Sle2.Sle3 (≈8 months, $n = 5$, $p = 0.0385$), B6·Sle1.Sle3 (10 months, $n = 7$, $p = 0.0002$), B6·Sle1.Yaa (8 months, $n = 5$, $p < 0.0001$), and B6.Lyn$^{-/-}$ (8 months, $n = 5$, $p < 0.0001$) but not B6·Sle3 (8 months, $n = 4$, $p = 0.2220$) mice. Error bars represent standard deviation. (B) Immunofluorescent stain of Axl

(green) and DAPI (blue) in the spleens of healthy B6 (top) and lupus-prone Mrl-lpr (bottom) mice. Axl appears on the surfaces of some B6 splenocytes but is absent from lupus-prone Mrl-lpr splenocytes (representative of three mice per strain). (C) Splenic Axl and (activated) Y779-phospho-Axl are significantly reduced in spleens of 6-month-old diseased Mrl-lpr mice versus age-matched B6 controls as measured by Western analysis ($p = 0.001$, 0.0015 on densitometry). (D) Axl is lost from the surface of CD11b+ and CD19+ B6·Sle1.Yaa splenocytes. B6 and B6·Sle1.Yaa spleens were harvested at 8 months. Splenocytes were stained for CD11b, CD19, CD8, CD4, and either A555-conjugated isotype control (red) or α-Axl antibody (blue). As expected and depicted in representative plots, B6 CD11b+ and CD19+ splenocytes stained positively for Axl. Conversely, B6·Sle1.Yaa splenocytes did not stain positively for Axl. Representative plots shown, $n = 3$ mice per group. Statistical analysis available in Supplemental Table 2. (E) Axl mRNA expression is unchanged in lupus-prone splenocytes versus age-matched healthy B6 control splenocytes by RT-PCR. Axl mRNA is shown in relative units versus Cyclophilin A loading control calculated by ΔCt ($n = 3$ mice per group in each of 3 separate experiments, one representative experiment shown; error bars represent standard deviation; see also see Ref [31], Fig. 2D).

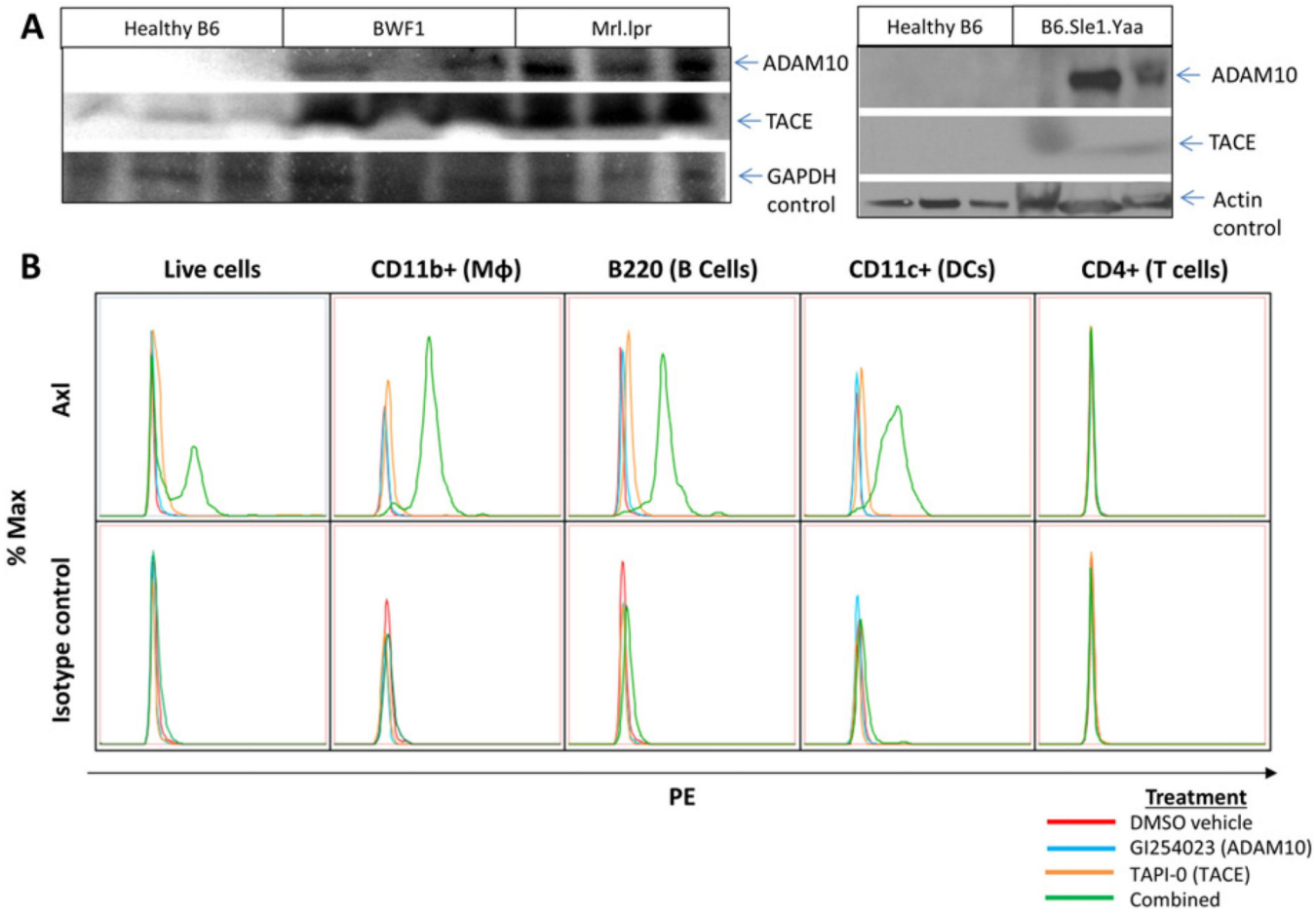

Fig. 3.

ADAM10 and TACE cleave Axl in lupus-prone leukocytes. (A) Matrix metalloproteases ADAM10 and TACE (ADAM17) are higher in lupus-prone BWF1 ($p = 0.019, 0.0429$), Mrl-lpr ($p = 0.0016, 0.0022$), and B6·Sle1.Yaa ($p = 0.0535, 0.0087$) splenocytes versus age-matched healthy B6 controls as shown by Western blot and quantified by densitometry. (B) B6·Sle1.Yaa splenocytes were isolated and treated for 18 h with DMSO vehicle control (red), 50 μM ADAM10-specific inhibitor GI254023 (blue), 50 μM TACE-specific inhibitor TAPI-0 (orange), or both inhibitors together (green) and analyzed with PE-conjugated anti-Axl antibody (top row) or isotype control (bottom row). Treatment with either inhibitor alone only slightly increases Axl staining, whereas combined treatment with both inhibitors rescues Axl surface staining on CD11b+, B220+, and CD11c+ splenocytes at 18 h. CD4+ splenocytes do not express Axl. Representative plots of four experiments are shown.

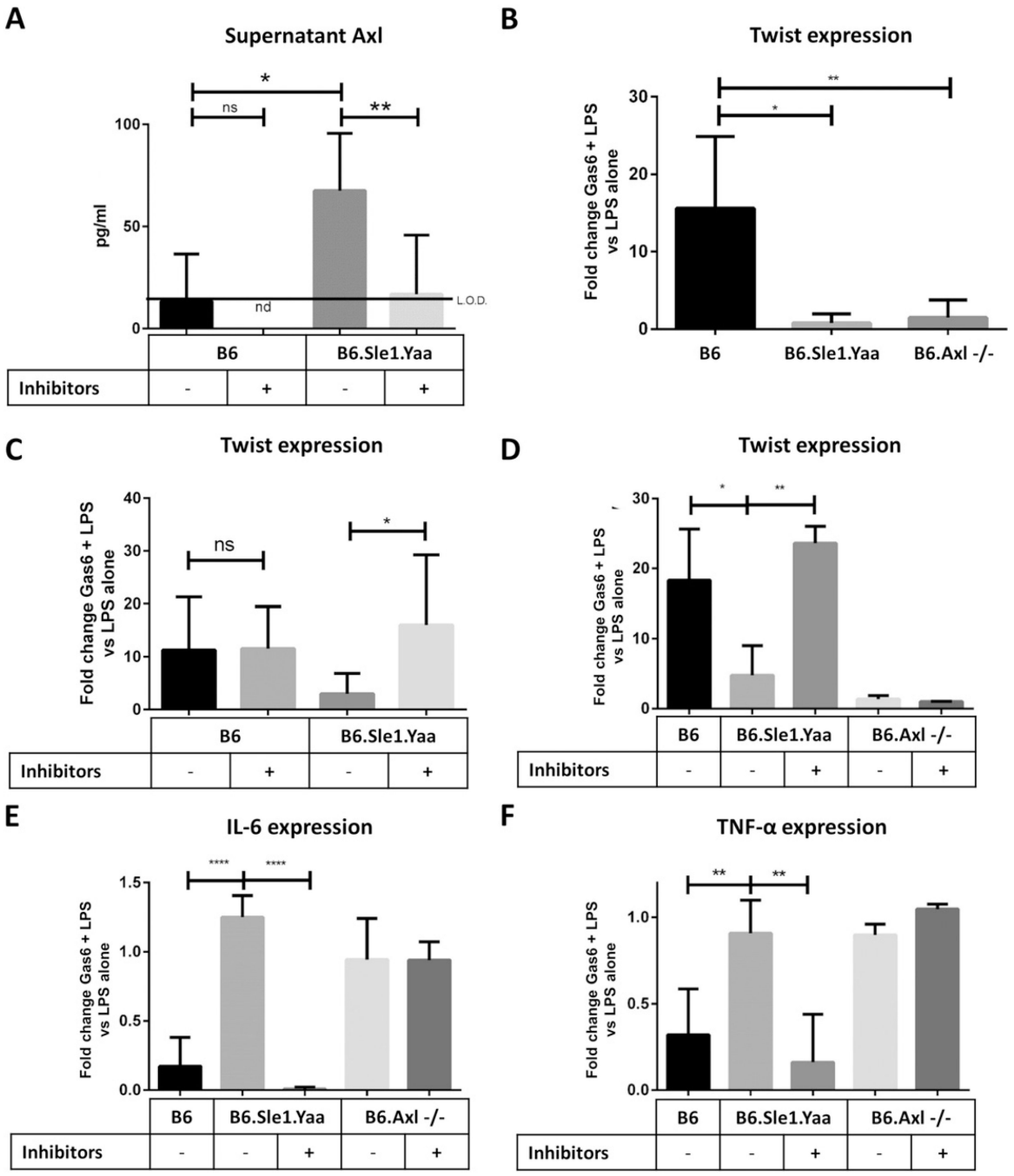

Fig. 4.

Lupus-prone splenocytes do not respond to Gas6 treatment unless Axl surface expression is rescued by ADAM10/TACE inhibition. (A) B6 and B6 · Sle1.Yaa splenocytes were isolated and treated for 24 h with DMSO vehicle control or 50 μM ADAM10 inhibitor GI254023 and 50 μM TACE inhibitor TAPI-0. After 24 h, supernatants were isolated and assayed for sAxl. B6·Sle1.Yaa supernatants contained higher sAxl levels than B6 wild-type controls (p = 0.0308) and treatment of B6·Sle1.Yaa splenocytes with protease inhibitors reduced supernatant sAxl levels to that of wild-type controls (p = 0.0027). (B) B6, B6·Sle1.Yaa, and

B6.Axl$^{-/-}$ splenocytes were isolated and treated with 1 ng/ml LPS alone or with both 1 ng/ml LPS plus 400 ng/ml Gas6 for 24 h. Twist expression was measured by RT-PCR and normalized to the Cyclophilin A loading control by ΔCt The ratio of Twist expression in Gas6 plus LPS-treated samples versus in LPS only-treated samples is shown. B6·Sle1.Yaa and B6.Axl$^{-/-}$ splenocytes do not upregulate Twist in response Gas6 (n = 5 total mice per group, analyzed in three separate experiments; *, p = 0.0113; **, p = 0.0035). (B and C) Splenocytes were isolated as above and pre-treated for 24 h with DMSO vehicle control or 50 μM ADAM10 inhibitor GI254023 and 50 μM TACE inhibitor TAPI-0. After 24 h, the cells were treated with 1 ng/ml LPS alone or with both 1 ng/ml LPS plus 400 ng/ml Gas6 for 24 h. Twist expression was then determined by RT-PCR as above and the ratio of Twist expression in Gas6 plus LPS-treated samples versus in LPS-treated samples is shown. B6·Sle1.Yaa splenocytes express Twist in response to Gas6 stimulation only when rescued by inhibition of ADAM10 and TACE (n = 5 mice per group; *, p = 0.0251; **, p = 0.0058). (E and F) Samples from C were also assayed for IL-6 (E) and TNF-α (F) expression by RT-PCR. The ratio of IL-6 and Tnf-α expression in Gas6 and LPS only-treated samples versus LPS-treated samples is shown. IL-6 and TNF-α expression are reduced in response to Gas6 in Sle1.Yaa splenocytes treated with ADAM10 and TACE inhibitors (n = 5 as in (B); ****, p < 0.0001; **, p < 0.01).

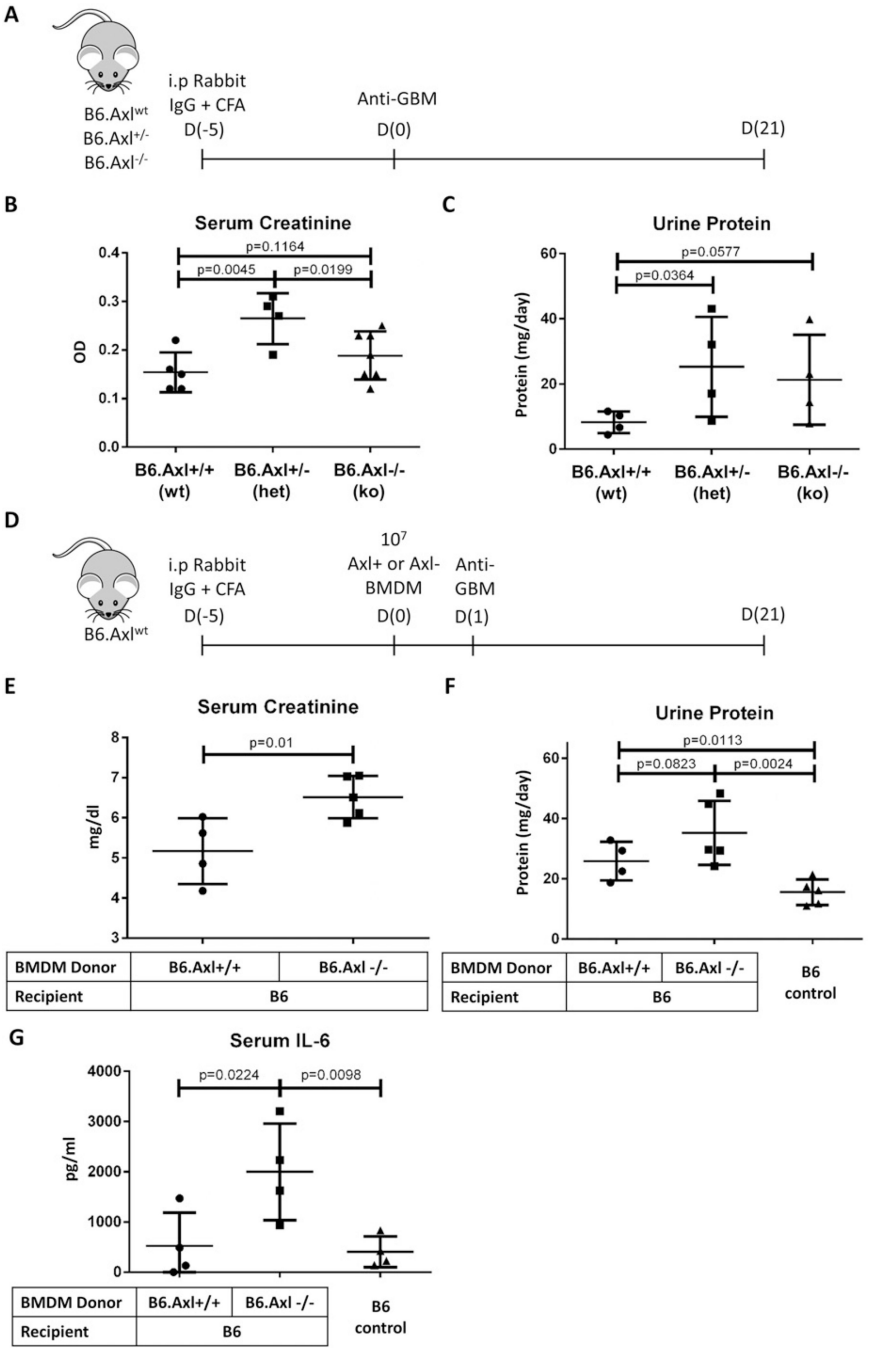

Fig. 5.

Macrophage Axl loss contributes to end-organ damage in a model of nephritis. (A–C) Anti-glomerular basement membrane (GBM) disease is induced in mice by D(−5) intraperitoneal injection of a 225 μl mixture of 100 μl complete Freund's adjuvant (CFA), 100 μl PBS, and 25 μl rabbit IgG, followed by an intravenous injection of mouse anti-rabbit glomerular basement membrane serum at 150 μl per 20 g body weight on D0 (A). Axl heterozygotes (het, $n = 4$) fared worse than Axl knockouts (ko, $n = 7$) or wild-type mice (wt, $n = 5$) as measured by serum creatinine (B) and proteinuria (C). (D–G) Anti-glomerular basement

membrane (GBM) disease is induced in mice by D(−5) intraperitoneal injection of a 225 μl mixture of 100 μl complete Freund's adjuvant (CFA), 100 μl PBS, and 25 μl rabbit IgG and D1 intravenous injection of mouse anti-rabbit glomerular basement membrane serum at 150 μl per 20 g. 10^7 cultured bone marrow-derived macrophages (BMDM) are injected at D0 (D). Axl-deficient BMDM recipients ($n = 5$) fared worse than Axl-sufficient BMDM recipients ($n = 4$) as measured by serum creatinine (E), upward-trending proteinuria (F), and elevated serum IL-6 levels (G). Error bars represent standard deviation. B6 controls did not receive anti-GBM induction. Additional data are shown in Supplemental Fig. 4.

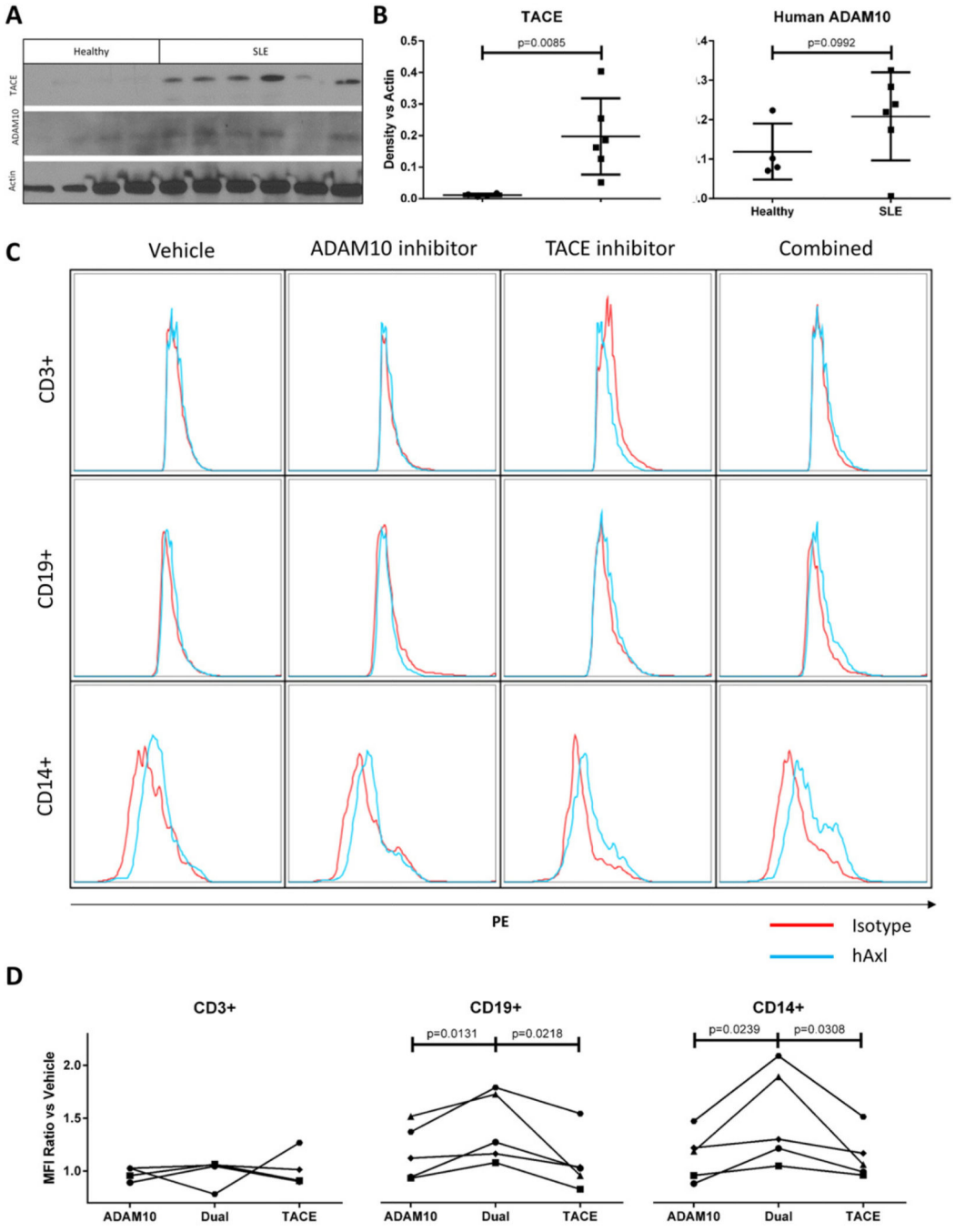

Fig. 6.

PBMCs from SLE patients upregulate Axl in response to combined protease inhibition. (A–B) PBMCs from healthy and SLE donors were isolated, extracted for protein, and probed for TACE and ADAM10 by Western analysis. Densitometric comparison versus actin control confirms TACE elevation in SLE PBMCs ($p = 0.0085$) with ADAM10 showing an upward trend on SLE PBMCs. (C) SLE patient PBMCs were treated for 18 h with DMSO vehicle control (column 1), 50 μM ADAM10-specific inhibitor GI254023 (column 2), 50 μM TACE-specific inhibitor TAPI-0 (column 3), or both inhibitors together (column 4). Cells were then

isolated and stained with PE-conjugated anti-Axl antibody (blue) or isotype control (red) plus anti-CD3, CD19, and CD14 antibodies and analyzed by flow cytometry. CD3+ cells did not stain for Axl. CD19+ and/or CD14+ SLE PBMCs showed increased Axl staining in samples treated with both protease inhibitors, which varied from patient to patient (rows 2–3, representative of five experiments). (D) Changes in Axl surface staining in response to protease inhibitor treatment were compared. We divided the difference between PE mean fluorescence intensity (MFI) of isotype control samples and corresponding Axl-stained samples by the difference in isotype control-stained and Axl-stained vehicle control-treated samples. MFI ratio = ((Axl-stained protease inhibitor-treated sample MFI) − (isotype control-stained protease inhibitor-treated sample MFI)) ÷ ((Axl-stained vehicle-treated sample MFI) − (isotype control-stained vehicle-treated sample MFI)). Thus a ratio of 1 means that there is no difference in Axl staining intensity in a given sample versus vehicle-treated control. This calculation was performed in CD3+, CD19+, and CD14+ subsets.